Effects of resonant excitation and stimulated emission in x-ray multiphoton ionization of neon atoms

Tanakrit Mamee, Chiang Mai University, Thailand

September 5, 2018

Abstract

The interaction between atoms and x-ray pulse, especially the very intense one, provides many interesting physics and fruitful features in various fields, for instance x-ray imaging. For investigating such phenomena, XATOM has been an essential tool to describe x-ray and atom interaction. In this work, we present the contribution of the resonant excitation and the stimulated emission process in x-ray multiphoton ionization in Ne atom by scanning photon energy and fluence of x-ray free electron laser pulses. We focus on the specific range of photon energy, where the hidden resonant excitation (1s→2p) plays an important role, and examine how stimulated emission influences the ionization dynamics involving resonant excitations. We found that in the energy regime corresponding to 1s–2p transition, the stimulated emission itself is non-negligible but it barely changes the overall shape of charge state distribution.

Contents

1 Introduction

The experimental and theoretical exploration of the interaction between matter and highly intense x-ray field was preliminary conducted in 2010 with the Linac Coherent Light Source (LCLS), the first facility of x-ray free-electron laser (XFEL) with kiloelectronvolt photon energies. From this study, the photoabsorption mechanisms and the electronics response of an atom in femtosecond scale to the ultra-intense, short-wavelength x-ray pulse were observed for the first time and this confirmed the successful modelling of the interaction between x-ray and atoms using a rate equation approach[1]. Successively, the investigation of the intense x-ray and atoms interaction with the 10-fs pulse duration showed the interesting nonlinear phenomena in photoabsorption process of Ne atom driven by hidden resonance excitation (1s→2p) forbidden in neutral neon[2]. In 2012, there was a study in high-Z Xe atom, suggesting the transient resonance-enhanced absorption mechanism, in resonance-enabled X-ray multiple ionization (REXMI), to be the main process producing unexpectedly high xenon charged states[3]. As the key mechanism in REXMI is creating more excited states and then allowing further ionization by Auger decay, the process of stimulated emission that countervails the excited states creation in resonant excitation needs to be accounted competing with the Auger decay process.

In this work, we feature the implementation of resonant excitations and stimulated emission in x-ray multiphoton multiple ionization dynamics. Scanning the photon energy and fluence of the XFEL pulse, we calculate charge state distributions (CSD) when the resonant excitation process is turned on and off in our rate-equation model. Also we simulate ionization dynamics including resonant excitations with and without stimulated emission at a specific photon energy, where hidden resonance emerges, in order to examine the effect of stimulated emission on ionization dynamics.

2 Theory

Consider a Ne atom imposed in the intense x-ray field, the initial interaction between the x-ray photons and electrons in Ne can be x-ray photoabsorption. Once the energy of such x-ray photons is sufficiently high for ionizing the core electrons, there are many interesting physics to study, such as relaxation process of filling of the inner vacancy by the electron from the upper subshell and emitting another electron, known as Auger decay and fluorescence decay. When the intensity of the x-ray beam is high enough, these processes happen sequentially. At high x-ray intensity, it is also possible to ionize another core electron before relaxation processes, yielding double-core-hole or multiple-core-hole states. All these processes result in the ionization of multiple electrons after absorbing many photons and this multiphoton multiple ionization mechanism has been discussed earlier in [4, 5, 6]. In this context, we will focus on the implementation of the resonant excitation and the stimulated emission in Ne atom ionization dynamics.

2.1 Resonance excitation

The resonance excitation is a process that allows a electron in ith subshell to be resonantly excited to another higher unoccupied jth subshell, when absorbing the energy corresponding to the energy difference between the initial and final states, as shown in Figure 1. This process can contribute for further ionization, especially by subsequent Auger decay from the core vacancy created after resonant excitation, if the ith subshell is core. Multiple resonant excitations can drive the processes to a pathway called resonance-enabled X-ray multiple ionization (REXMI)[3]. In XATOM the resonance excitation is implemented into the ionization dynamics process based on Monte Carlo rate equation approach by considering the transition between available configurations in the rate equation calculation, the resonant excitation cross section from ith to jth subshell $\sigma_{RE}(i,j)$ by a photon energy ω is given by [6],

$$\sigma_{RE}(i,j) = \frac{4}{3}\pi^2 \alpha \Delta E_{ji} N_i N_j{}^H \frac{l_>}{2(2l_i+1)(2l_j+1)} \times |\langle u_{n_j l_j}|r|u_{n_i l_i}\rangle|^2 \delta(\omega - \Delta E_{ji}), \quad (1)$$

where α is the fine structure constant, ΔE_{ji} is the transition energy between jth and ith subshell, l_i and l_j are the orbital angular momentum of ith and jth subshell, respectively, and $l_>$ is the greater of l_i and l_j. N_i and $N_j{}^H$ are the number of electrons in ith subshell and the number of holes in jth subshell, respectively.
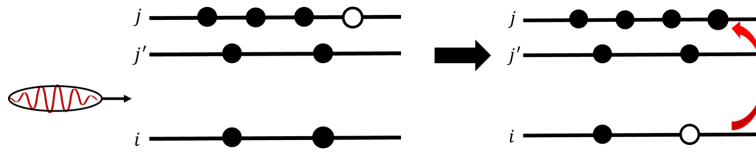
Figure 1: The diagram showing the resonant excitation process

2.2 Stimulated emission

The stimulated emission is another process that occurs when an electron in the excited state jth, influenced by an incident photon comes down to the lower energy level ith with the releasing photon carrying the same amount of the incident photon energy, where the process can be seen in Figure 2. This makes the stimulated emission capable to reduce the excited state population. The reduced excited state population contributes to the decreasing of Auger decay, which prevents the system to be further ionized by Auger decay process. The cross section of the stimulated emission from jth subshell to ith subshell $\sigma_{SE}(j,i)$ can be written in term of the resonant excitation cross section from ith to jth subshell as,

$$\sigma_{SE}(j,i) = \frac{N_i'^H N_j'}{N_i N_j{}^H}\sigma_{RE}(i,j). \quad (2)$$

The $N_i'^H$ and N_j' are the number of holes in ith subshell and the number of electrons in jth subshell, respectively, after resonant excitation.
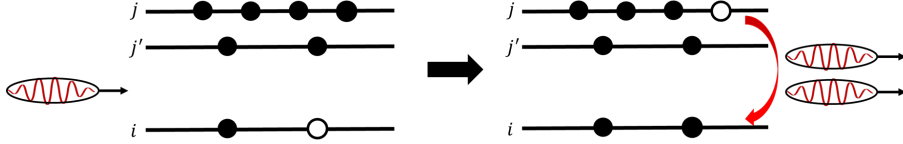
Figure 2: The diagram showing the stimulated emission process

3 Results and discussions

In this part, we study the ionization dynamics of Ne interacting with an intense x-ray pulse with 30 fs FWHM. In order to search the most appropriate beam parameters to investigate the role of resonant excitation and stimulated emission, we calculate charge state distributions (CSDs) varying the photon energy and fluence. Here we display the comparison of CSDs between resonance and non resonance cases. The CSDs are calculated using Monte-Carlo-on-the fly method using in XATOM with 1,000 trajectories for each data point of the photon energy and fluence. For the last section, we present how stimulated emission comes to play in such a resonance dominating condition by computing CSDs including the simulated emission cross section. For the numerical calculation in this work, we used 200 radial grid points for $0 \le r \le 100$ a.u. The maximum numbers for the principal quantum number n and the orbital angular momentum quantum number l were $n_{max} = 10$ and $l_{max} = 2$, respectively. For resonant excitation and stimulated emission calculations, the energy bandwidth of 5.25 eV was used.

3.1 Domination of resonance excitation in specific experimental condition

Firstly, we calculate the mean charge from CSDs with varying fluence and photon energy. Figures 3(a) and (b) show 3D contour map of the mean charge as a function of photon energy (x axis) and fluence (y axis). The results do not show the obviously distinguishable patterns between non-resonance(a) and resonance(b) cases.
To get the better insight where the resonance excitations occur, we plot the resonance excitation occurrence calculated from the Monte-Carlo methods in XATOM as shown in Figure 3(c). From the plot, we can see that only some range of photon energies allow resonance excitation to occur.
To specify the beam parameters where the resonant excitation becomes dominant, final charge state population for individual charge states are plotted for different beam fluence and photon energy in Fig. 4. (a) and (b) are for +4, (c) and (d) are for +6, and (e) and (f) are for +7. From the plot, one can see some population differences between resonance and non resonance cases, according to the resonant excitation occurrence plotted in Figure 3(c). The dominating resonant transition can be highlighted by matching the photon energies with the calculated transition energies for each charged states as shown in Figure 6. By matching the individual calculated ion yield plot in Figure 4 and transition energy in Figure 6, we observed that the resonant transition from K-shell and
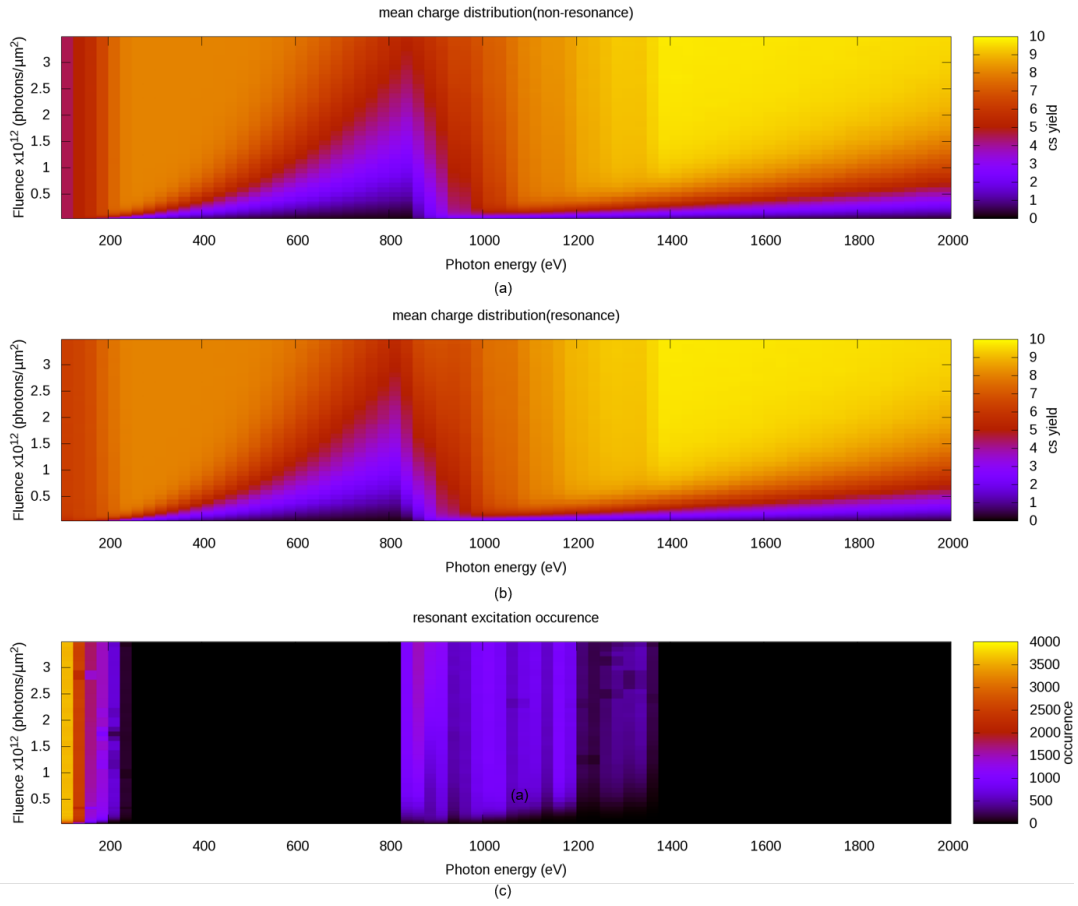
Figure 3: (a) the mean charge distribution for different beam parameters in non-resonance case (b) the mean charge distribution for different beam parameters in resonance case (c) the resonant excitation occurrence for different beam parameters

L-shell to higher shell contributes to the distinguishable difference between resonance and non-resonance cases around 0-300 eV energy regime (refers to L-shell transition) and 900-1300 eV energy regime (refers to K-shell transition). To simplify the situation, we pick up the case of the K-shell transition to study, even though there are less resonant excitation paths to consider. In Fig. 5, we increase the resolution of the map and zoom into the interval from 800 to 1100 eV by tuning the photon energy scan in order to do a further investigation on the resonant transition from K-shell, precisely 1s to 2p transition. In figure 5(a), it shows that the regime at the energy around 900 eV to less than 1000 eV is crowded for Ne^{4+} in non-resonance case, but once we include the feature of resonant excitation as shown in the figure 5(b), there is a fading of the +4 ion yield in the same regime because, at that energy regime, the charge state of +4 can be excited from K-shell to another according to some examples of the transition energy in the map in figure 6. We can see that many resonant excitation pathways can contribute in the situation, for instance, 1s to 3p, 1s to 4p, 1s to 5p and so forth. In the similar case in figure 5(c) and 5(d), the yield of +6 shows the same behaviour since there is a crowd of Ne^{6+} around 1000 eV to 1050 eV in the non-resonance case and partially disappears in the resonance case. Comparing to the transition energy of +6, those partially disappearance indicates the discontinuity of the transition energy between 1s–3p (998 eV) and 1s–4p (1034 eV) transition which contributes to the existence of the crowd of Ne^{6+} between the gap of those energy difference. We can also see that the Ne^{6+} is excited and get into higher charge state from considering the rising up of the Ne^{7+} yield [Fig. 5(f)] and the fading away of Ne^{6+} yield [Fig. 5(d)] in the same energy regime.

Nevertheless, we cannot see that the transition between 1s and 2p subshell (hidden resonant excitation) plays any role in this way because there is no remarkable yield difference between two cases at the energy near that transition(840-900 eV). It is suspected that the resonance feature is washed out because of a wide x-ray pulse bandwidth.
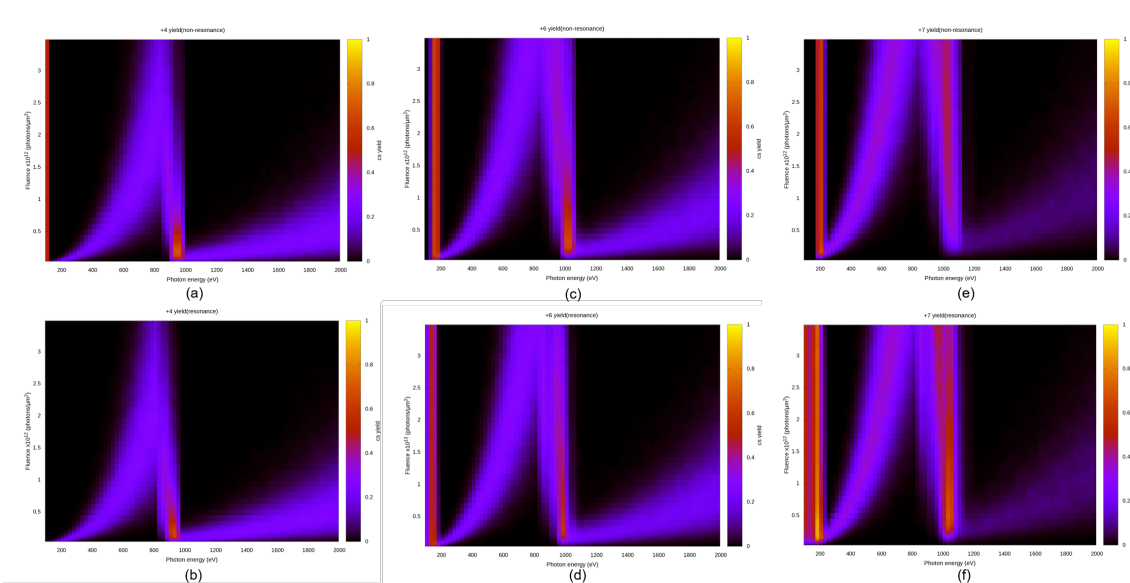
Figure 4: Ion yield spectra for individual charge states (+4, +6, and +7). The photon energy in the x axis ranges from 100 eV to 2000 eV. The fluence in the y axis ranges from zero to $3.5 \times 10^{12} ph/\mu m^2$.(a) Ne^{4+} for non-resonance case (b) Ne^{4+} for resonance case (c) Ne^{6+} non-resonance case (d) Ne^{6+} for resonance case (e) Ne^{7+} for non-resonance case (f) Ne^{7+} charge state Ne for resonance case

3.2 Implementation of stimulated emission in X-ray photoionization

Despite of no clear evidence of hidden resonance in CSD plots in the previous section, we would like to see the effect of stimulated emission on the 1s→2p resonant excitation, because a) the dipole matrix element between 1s and 2p is the largest one and b) it does not increase the number of subshells to be excited, thus it does not increase configurational space in ionization dynamics calculations. To maximize the resonant excitation cross section, we fixed the photon energy at 840 eV that is nearby the 1s-2p transition energy for Ne^{1+} and Ne^{2+}. We calculate the charge state distribution including both resonant excitation and stimulated emission. The fluence-dependent CSDs are calculated to compare with three cases; non-resonance, resonance without stimulated emission and resonance with stimulated emission. In figure 7, the contour map of CSDs shows that there is an obvious difference in pattern between resonance and non-resonance cases but it is still hard to see such a difference between resonance cases with and without stimulated emission. To obtain a clearer picture, we pick up some specific fluence cases and plot the CSDs for each case as shown in figure 9. Focusing the resonance cases with and without stimulated emission case, We can see that there is a difference between the interval of 0.8-0.9 $\times 10^{12} photon/\mu m^2$ but overall two curves are very similar and the difference diminishes when CSDs are pushed to high charge states as fluence increases. In addition, we can also see that the stimulated emission contributes in decreasing of the maximum charged state compared to those from resonance case

8
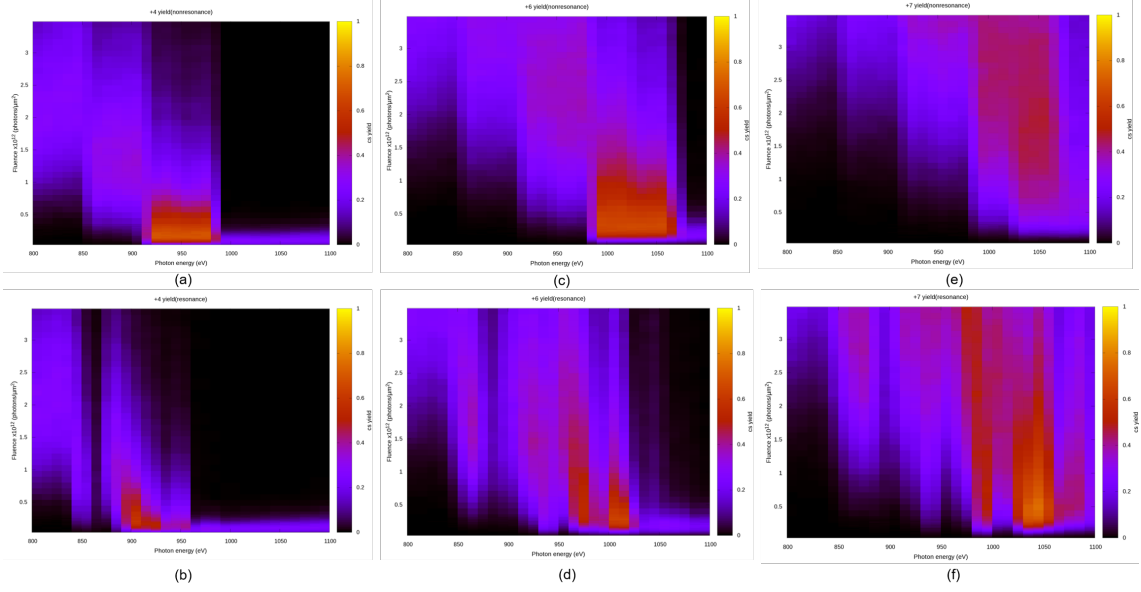
Figure 5: Zoomed-in spectra of Figure 4. The photon energy in the x axis ranges from 800 eV to 1100 eV and the energy step is 25 eV. (a) Ne^{4+} for non-resonance case (b) Ne^{4+} for resonance case (c) Ne^{6+} non-resonance case (d) Ne^{6+} for resonance case (e) Ne^{7+} for non-resonance case (f) Ne^{7+} for resonance case

since the stimulated emission process can reduce the population of excited state Ne and prevent the Auger decay process, which is the main process to obtain the higher charge states in the resonance case. In Figure 8, the Auger decay rate and the maximum stimulated emission rate at a given fluence with a pulse duration of 30 fs FWHM are plotted together for relevant electron configurations to find the critical fluence that allows the stimulated emission to overcome the Auger decay and to be dominating. From the plot, we found that the stimulated emission becomes dominant at very low fluence regime about 4×10^{10} $ph/\mu m^2$ in these specific cases of Ne^{1+} and Ne^{2+}. However, the inclusion of stimulated emission does not change that much the charge state distribution as shown in Figure 9, because resonance occurs only at +1 and +2, not at other charge states. Anyhow, this finding indicates a non-negligible feature of stimulated emission in the model of XFEL-atom interaction.
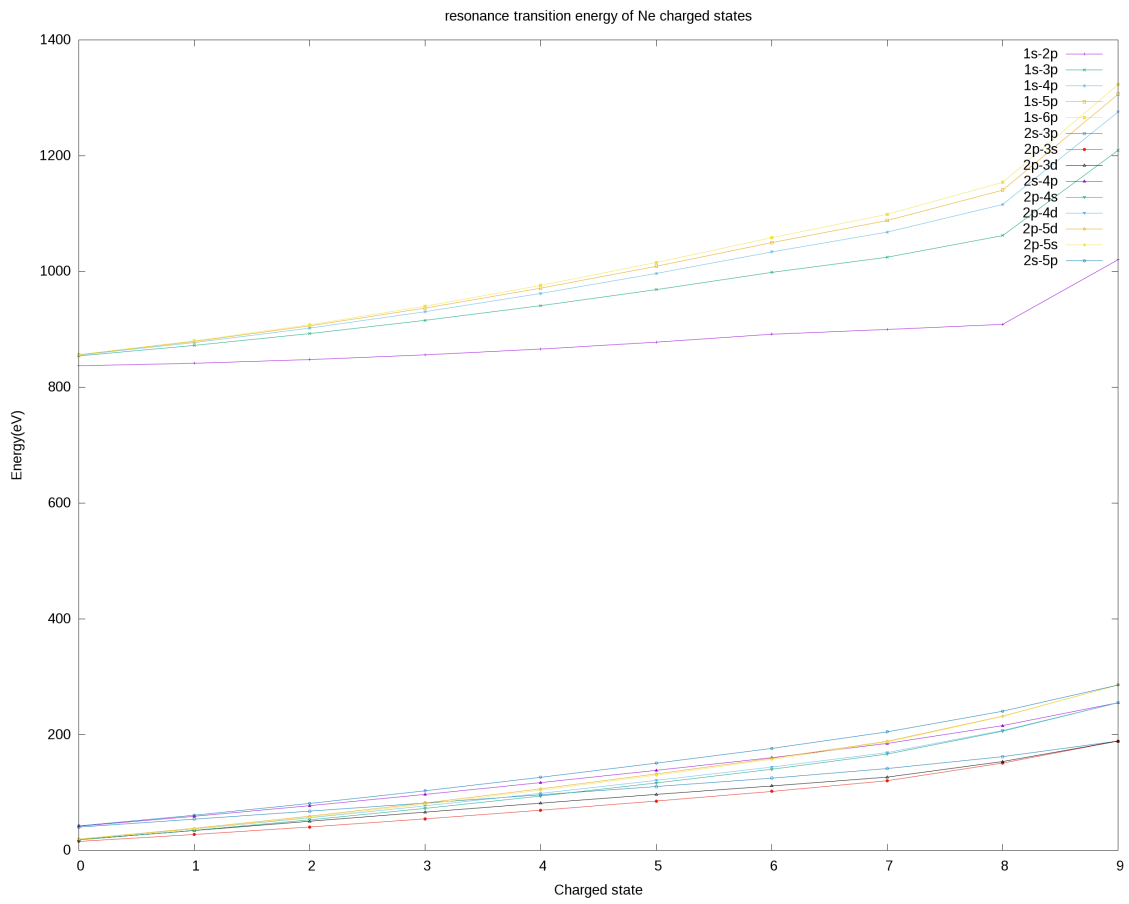
Figure 6: The plot of each resonant transition energy of different Ne charge states
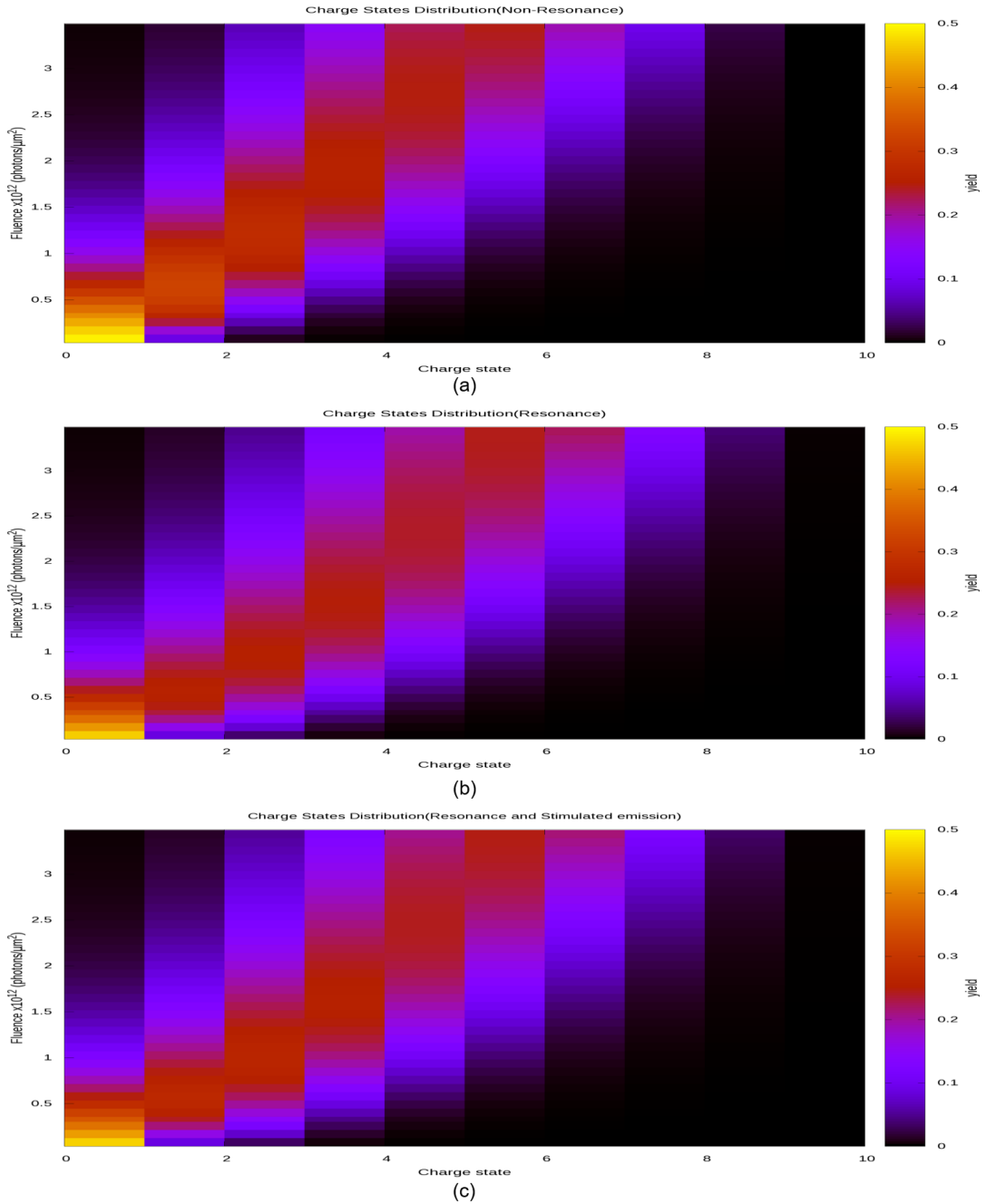
Figure 7: The contour plot of charge state distribution for non-resonance case(a), including resonance case(b), and including stimulated emission case(c) as a function of beam fluence (y-axis). The photon energy is fixed at 840 eV.
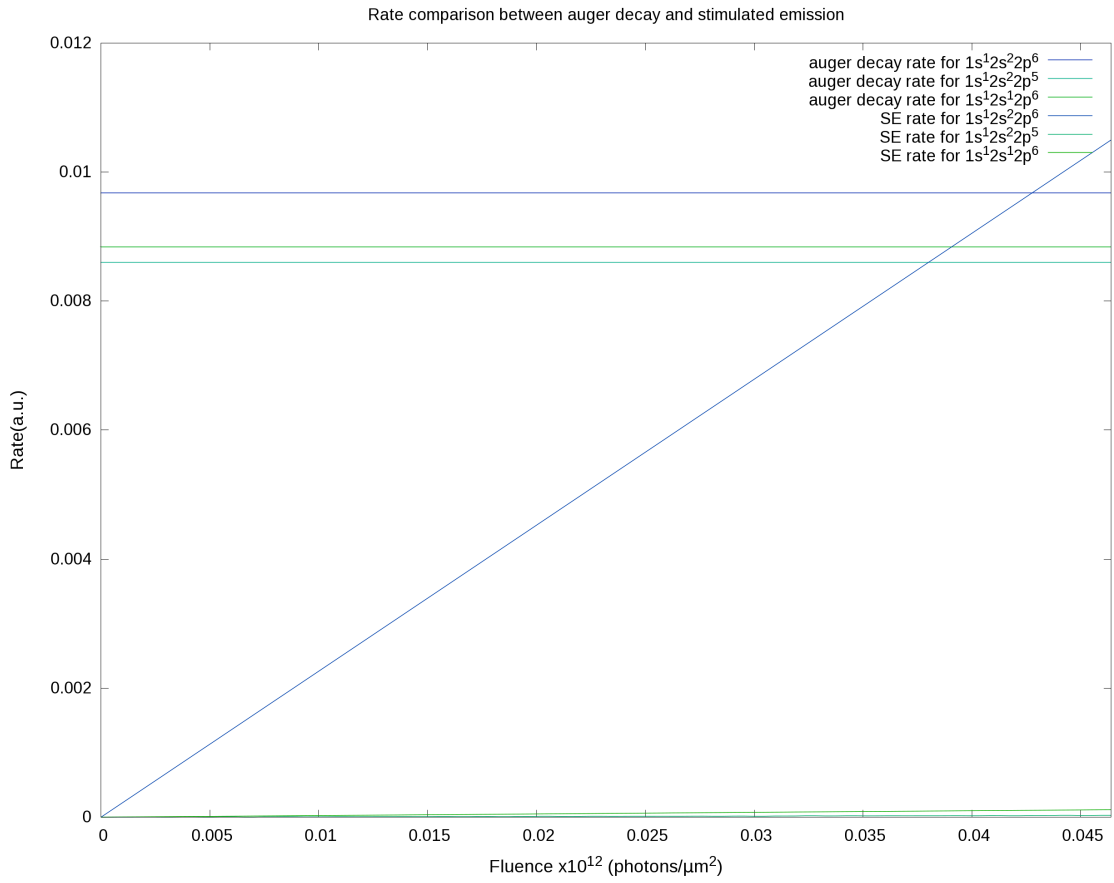
Figure 8: The Auger decay rate and stimulated emission rate for each individual electronic configuration as a function of fluence. The photon energy is fixed at 840 eV.
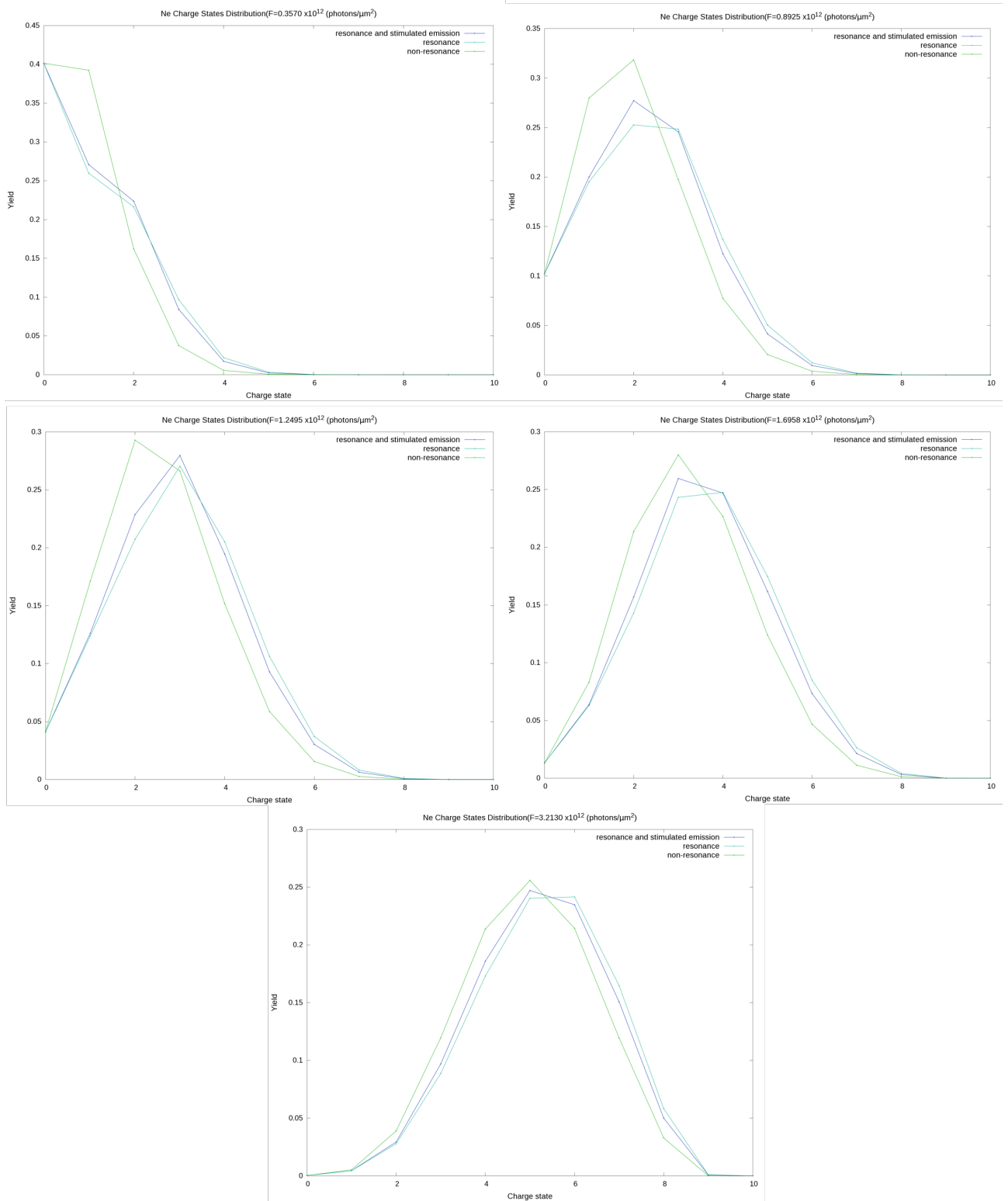
Figure 9: The charge state distribution with different fluence conditions

4 Conclusion

In this work, we found that resonant transitions influence the ionization dynamics and resulting charge state distributions. We apply the stimulated emission to the existing rate-equation model in the energy regime near the 1s–2p transition that is forbidden in neutral Ne. From this study, we found that the implement of stimulated emission itself is non-negligible even in very low fluence regime; however, it does not modify the overall shape of charge state distribution because the resonant condition is satisfied at only a few charge states. Therefore, it should be interesting to see how stimulated emission influences the ionization dynamics in REXMI[3], where a range of charge states meet the resonance condition simultaneously.

References

[1] L. Young *et al.*, Femtosecond electronic response of atoms to ultran-intense X-rays. *Nature(London)* **466**, 56 (2010)

[2] E. P. Kanter *et al.*, Unveiling and Driving Hidden Resonances with High-Fluence, High-Intensity X-Ray Pulses. *Phys. Rev. Lett.* **107**, 233001 (2011)

[3] Benedikt Rudek, Sang-Kil Son, Daniel Rolles *et al.*, Ultra-efficient ionization of heavy atoms by intense X-ray free-electron laser pulses. *Nature Photon.* **6**, 858-865 (2012)

[4] Robin Santra, Concepts in x-ray physics. *J. Phys. B: At. Mol. Opt. Phys.* **42**, 023001 (2009)

[5] Sang-Kil Son, Linda Young, and Robin Santra, Impact of hollow-atom formation on coherent x-ray scattering at high intensity. *Phys. Rev. A* **83**, 033402 (2011)

[6] Koudai Toyota *et al.*, Interplay between relativistic energy corrections and resonant excitations in x-ray multiphoton ionization dynamics of Xe atoms. *Phys. Rev. A* **95**, 043412 (2017)